Published in final edited form as:
Biochem Biophys Res Commun. 2007 April 6; 355(2): 324–330.

Cytoskeleton dynamics: fluctuations within the network

Predrag Bursac[1,2,§], **Ben Fabry**[3], **Xavier Trepat**[1], **Guillaume Lenormand**[1], **James P. Butler**[1], **Ning Wang**[1], **Jeffrey J. Fredberg**[1], and **Steven S. An**[1,4,§]

1 *Molecular and Integrative Physiological Sciences, Department of Environmental Health, Harvard School of Public Health, Boston, MA 02115*

2 *Sports Medicine Group, Regeneration Technologies Inc., Alachua, FL 32616*

3 *Department of Physics, Erlangen University, Erlangen, Germany*

4 *Division of Physiology, Department of Environmental Health Sciences, Johns Hopkins Bloomberg School of Public Health, Baltimore, MD 21205*

Abstract

Out-of-equilibrium systems, such as the dynamics of a living cytoskeleton (CSK), are inherently noisy with fluctuations arising from the stochastic nature of the underlying biochemical and molecular events. Recently, such fluctuations within the cell were characterized by observing spontaneous nano-scale motions of an RGD-coated microbead bound to the cell surface (Bursac et al., *Nature Mat.* 2005;4:557–561). While these reported anomalous bead motions represent a molecular level reorganization (remodeling) of microstructures in contact with the bead, a precise nature of these cytoskeletal constituents and forces that drive their remodeling dynamics are largely unclear. Here we focused upon spontaneous motions of an RGD-coated bead and, in particular, assessed to what extent these motions are attributable to (i) bulk cell movement (cell crawling), (ii) dynamics of focal adhesions, (iii) dynamics of lipid membrane, and/or (iv) dynamics of the underlying actin CSK driven by myosin motors.

Keywords

Cytoskeleton; Remodeling; Lipid Dynamics; Airway Smooth Muscle

INTRODUCTION

The cytoskeleton (CSK) is fundamental to many cellular processes, including proliferation, migration, and contraction [7,20,21]. To perform these functions, cells orchestrate a complex cascade of signals and molecules that lead to robust structural changes in the underlying CSK [15,21]. This ability of the CSK to disassemble, to reform, and to stabilize provides, for example, a basic framework for metastasis of a cancer cell as it explores, crawls, and invades other tissues [5,41,45]. As such, progression of cancer as well as pathogenesis of many chronic disorders is now thought to be associated with abnormalities in the stability and dynamics of the underlying CSK [16,34,37,39].

Corresponding author: Steven S. An, Ph.D., Johns Hopkins University, Bloomberg School of Public Health, 615 N. Wolfe Street, Room E-7616, Baltimore, MD 21205, Tel.: (410) 502-5085, Fax: (410) 955-0299, Email: san@jhsph.edu.
§These authors contributed equally to this work

The CSK is a network of actin, microtubules, and intermediate filaments that are bound together by associated cross-linkers and driven by motor proteins [8,21,27]: the cell interior is a crowded environment [11,12] and, at the same time, is far from an equilibrium system [18]. Such complexity of the network and its out-of-equilibrium dynamics are the focus of much attention in the fields as diverse as condensed matter physics [10,17,28] as well as biophysics of the living cell [13,25,26,35,38,42]. Most recently, we have made a series of phenomenological observations in a number of different cell types and reported a functional assay that probes molecular level fluctuations within the living cell [1,3,6]. This assay is based on spontaneous nano-scale movements of an individual microbead that is coated with a peptide containing the sequence Arg-Gly-Asp (RGD); such beads bind to cell surface integrin receptors [43], form focal adhesions [29,30], and become well-integrated into the cytoskeletal scaffolding [13,19, 29,33]. Accordingly, these bead motions may reflect ongoing remodeling events of the underlying cytoskeletal network [1,3,6], but the structural origin of such motions and forces that drive these dynamics in a living cell remain to be elucidated.

Like the CSK of many cell types, that of the airway smooth muscle (ASM) cell is a dynamic structure that is in a continuous state of remodeling [1,4,6,24,31,39]. Using the ASM cell as a model and, using multiple well-defined cell microenvironments, we provide here strong evidence that spontaneous nano-scale motions of an individual RGD-coated microbead report ongoing molecular level reorganization of the underlying actin CSK driven by myosin motors.

MATERIALS AND METHODS

Materials

Tissue culture reagents were obtained from Sigma (St. Louis, MO). The synthetic Arg-Gly-Asp (RGD) containing peptide was purchased from American Peptide Company, Inc. (Sunnyvale, CA) and acetylated low-density lipoprotein (acLDL) was purchased from Biomedical Technologies (Stoughton, MA). The micropatterned (50 μm × 50 μm) substrates were a generous gift from Dr. Phillip DeLuc (Boston, MA). All other reagents and drugs were obtained from Sigma with the exception of jasplakinolide which was purchased from CalBiochem (La Holla, CA). Jasplakinolide and cytochalasin-D were prepared in sterile dimethylsulfoxide (DMSO). Histamine and N^6,2′-O-dibutyryladenosine 3′,5′-cyclic monophosphate (db-cAMP) were reconstituted in sterile distilled water. On the day of experiments, all drugs were diluted to final concentrations in serum-free media, yielding less than 0.1 % DMSO in final volume.

Cell culture

Human ASM cells were provided by Dr. Reynold Panettieri (University of Pennsylvania, PA) and rat ASM cells were prepared as previously described [1,2]. Cells were grown until confluence at 37°C in humidified air containing 5 % CO_2 and passaged with 0.25 % trypsin-0.02 % EDTA solution every 10–14 days. In the present study, we used cells in passages 3–7. Unless otherwise specified, serum-deprived post-confluent cells were plated at 20,000 cells/cm^2 on plastic wells (96-well Removawell, Immulon II: VWR International, West Chester, PA) previously coated with type I collagen (Vitrogen 100; Cohesion, Palo Alto, CA) at 500 ng/cm^2. Cells were maintained in serum-free media for 24 h at 37°C in humidified air containing 5 % CO_2. These conditions have been optimized for seeding cultured cells on collagen matrix and for assessing their mechanical properties [2,13,43].

Bead coating

Ferrimagnetic microbeads were coated with RGD, acLDL or PLL as described previously [9, 13,33,43]. Unless otherwise noted, approximately 5×10^4 beads were added to individual

sample wells and incubated for 20 min. Unbound beads were then removed by washing cells with serum-free media.

Characterization of spontaneous bead motions

Under microscopic observation, we visualized spontaneous displacements of an individual microbead (approximately 40 to 100 beads per field-of-view) and recorded its positions at frequency of 12 frames/s for t_{max} ~ 330 s as previously described [6]. Bead positions were corrected for the effects of microscope stage drift; the stage drift was estimated from changes in the mean position of all beads within a field of view [6]. We defined mean square displacement (MSD) of an individual bead as

$$MSD_b\langle\Delta t\rangle = \langle(r(t+\Delta t) - r(t))^2\rangle \quad (1)$$

where $r(t)$ is the bead position at time t, Δt is the time lag, and brackets indicate an average over many starting times t [6]. The limit of resolution in our system was on the order of ~ 10 nm, but for $\Delta t \sim 4$ s most beads had displaced a much greater distance. Accordingly, we analyzed data for time lags greater than 4 s and up to t_{max}. MSD of most beads increased with time according to a power law relationship.

$$\mathrm{MSD}\langle\Delta t\rangle = D*(\Delta t/\Delta t_o)^{\alpha} \quad (2)$$

The coefficient D^* and the exponent α of an individual bead were estimated from a least-square fit of a power-law to the MSD data for Δt between 4 s and $t_{max}/4$. The upper cut-off of $t_{max}/4$ was chosen arbitrary to increase statistical accuracy of estimated D^* and α. We took Δt_o to be 1 s and expressed D^* in units of nm^2.

In the present study, we quantified individual bead motions both before and after each drug treatment by MSD(Δt). To modulate actin polymerization, cells were treated for 30–60 min with actin disrupting agent cytochalasin-D (1 μM) or for 10 min with actin polymerizing agent jasplakinolide (1 μM). To modulate actomyosin interactions, cells were contracted for 5 min with histamine (100 μM) or relaxed for 15 min with db-cAMP (1 mM).

Optical magnetic twisting cytometry (OMTC)

To estimate the stiffness of structures bound to the bead, we measured bead displacements under applied torque as previously described [13]. In brief, ferrimagnetic microbeads were first magnetized horizontally (parallel to the surface on which cells were plated) and then twisted in a vertically aligned homogenous magnetic field (20 Gauss) at a frequency of 0.75 Hz. The resulting lateral bead displacements in response to the oscillatory torque were detected optically, and the ratio of specific torque to lateral bead displacements was computed and expressed as the cell stiffness in units of Pa/nm.

RESULTS AND DISCUSSION

Characterization of spontaneous bead motions

Spontaneous motions of each RGD-coated bead (4.5 μm in diameter) bound to the surface of the ASM cell were random and consisted of relatively small steps (Figure 1A); over the course of 5 min, bead trajectories amounted to only a small fraction of the bead diameter. Such trajectories, however, appeared elongated or directed, suggesting a certain degree of positive correlation between incremental bead steps.

For each bead, we characterized its spontaneous nano-scale motions by calculating mean square displacement (MSD_b) (Equation 1); MSD_b varied by two orders of magnitude, but MSD_b of most beads increased with time according to a power law relationship (Figure 1B).

These motions were further characterized by fitting a power-law to individual MSD_b to estimate diffusion coefficient D* and the exponentα. The probability density of the diffusion coefficient D*, between individual beads, showed monophasic and almost lognormal distributions with a maximum of 50 nm^2, whereas that of the exponent α exhibited monophasic and almost normal distributions with a maximum of 1.6 (Figure 1C). Accordingly, ensemble average of all MSD_b (MSD) demonstrated superdiffusive behavior (α> 1), whereby the MSD increased with time as ~ $t^{1.6}$ (Figure 1B: inset). Taken together, unlike a simple diffusive thermal Brownian motion that increases its MSD linearly with time [23], spontaneous motions of an individual RGD-coated bead were non-thermal in nature and, instead consistent with the notion that these anomalous motions are governed by an additional source of energy in the living cell [6].

Role of bulk cell movement (cell crawling)

We considered the possibility that these anomalous motions of an RGD-coated bead might be dictated by the motions of an entire cell body. To test this hypothesis, we used a micropatterned substrate on which a cell could adhere but not crawl [32]. Consistent with spontaneous bead motions on the sub-confluent cells, an RGD-coated bead attached to a serum-deprived cell seeded on a micropatterned substrate exhibited the same superdiffusive motions (Figure 1D). Thus, these findings suggest that cell crawling is at best a minor contributing factor for the observed anomalous bead motions.

Role of lipid membrane dynamics

To assess the relative contribution of cortical membrane dynamics, we used beads coated with acetylated low-density lipoproteins (acLDL); acLDL-coated beads bind to scavenger receptors thought to be floating in the cell membrane and, as such, are not linked avidly to the cytoskeletal structures deep in the cell interior [1,43]. The spontaneous motions of an acLDL-coated bead were remarkably different from motions of an RGD-coated bead (Figure 2A). Compared with motions of an RGD-coated bead, motions of an acLDL-coated bead consisted of relatively large incremental steps (bigger D*) that seemed to be uncorrelated in time (α~ 1).

In addition, acutely depleting cholesterol from the lipid membrane with methyl-β-cyclodextrin [22] increased membrane stiffness as probed by OMTC with an acLDL-coated bead (Figure 2B) and, at the same time, greatly reduced spontaneous lateral mobility of that same bead (Figure 2A). Cholesterol depletion did little to CSK stiffness and spontaneous motions of an RGD-coated bead, however (Figure 2). Accordingly, superdiffusive behavior of a RGD-coated bead seems to be insensitive to the dynamics of lipid membrane.

Effect of ligand coating density

Spontaneous motions of a bead (RGD versus acLDL) were also differentially affected by the amount of the ligand coating (0.1 to 300 ng/mg bead). Increasing coating density of RGD led to a dose-dependent increase in stiffness (G′) as measured by OMTC and, at the same time, caused systematic changes in its spontaneous bead motions; in this concentration range (0.1 to 300 ng/mg bead), the diffusion coefficient D* decreased by an order of magnitude whereas the exponent α increased from nearly diffusive behavior (slope ~ 1.0) to a highly superdiffusive behavior (slope ~ 1.7) (Figure 3A). In contrast, increasing coating concentration of acLDL did not yield appreciable changes in G′, D*, and α; in fact, these values were similar to those of the smallest amount of RGD coating (Figure 3A).

These findings are consistent with the notion that a bead with the smallest amount of RGD coating binds to individual or just a few integrin receptors and therefore may not be firmly anchored to the deep CSK [14]. In that case, motions of such bead on the living cell may report instead dynamics of lipid membrane, at best cortical actin, similar to that measured with an

acLDL-coated bead. On the other hand, the more firmly anchored a bead is to the underlying CSK deep in the cell interior (for example, the highest amount of RGD coating), the higher stiffness (G′) of that bead would be and, as a consequence, its spontaneous motions would exhibit smaller incremental bead steps (D*) while show faster and more correlated dynamics of its remodeling (higher α) (Figure 3B).

Role of focal adhesion dynamics

We next considered a potential link between such anomalous bead motions and the dynamics of focal adhesions and, accordingly, quantified spontaneous motions of an individual bead coated with poly-L-lysine (PLL). A PLL-coated bead does not form focal adhesions [4,36] but, similar to an RGD-coated bead, binds tightly to the underlying CSK [9]; stiffness (G′) as probed by OMTC with a PLL-coated bead was not appreciably different from that measured with an RGD-coated bead (Figure 3C).

As observed with an RGD-coated bead, spontaneous motions of an individual PLL-coated bead showed the same superdiffusive behavior; the computed D* and α were not statistically different from that of an RGD-coated bead (Figure 3C). These findings suggest that superdiffusive bead motions may report, rather than discrete changes in focal adhesions, underlying dynamics of the cytoskeletal structures deep within the cell.

Characterization of actin versus myosin modulations

To further quantify the relative contributions of actin and myosin motors to spontaneous bead motions, we used a panel of agencies that modulate their actions; we focused here upon actin and myosin because intermediate filaments and microtubules play little role in cell mechanics probed through an RGD-coated bead [1,40]. To modulate actin dynamics we used jasplakinolide and cytochalasin-D whereas to modulate myosin motors we used histamine and db-cAMP.

On the one hand, decreasing actin polymerization and disrupting actin stress fibers with cytochalasin-D as well as turning off myosin motors with db-cAMP led to an increase in D* and a decrease in α (Figure 4). On the other, increasing actin polymerization and actin stress fiber stabilization with jasplakinolide as well as turning on myosin motors with histamine resulted in a decrease in D* and an increase in α (Figure 4). Both actin polymerization and myosin activation are reported to increase tension within the CSK network whereas actin depolymerization and myosin inhibition decrease such tension [6,26,44]. Consistent with this notion, changes in the computed D* and α were closely correlated with changes in tension within the CSK. Taken together, these data provide strong evidence that anomalous motions of an RGD-coated bead on the cell surface are largely attributable to discrete molecular level remodeling events of the underlying actin CSK driven by myosin motors.

Acknowledgements

This study was supported by National Heart, Lung, and Blood Institute grants HL-59682 and HL-33009.

Abbreviations

ASM
: airway smooth muscle

CSK
: cytoskeleton

MSD
: mean square displacement

acLDL

acetylated low-density lipoprotein

PLL

poly-L-lysine

RGD

arginine-glycine-aspartic acid

References

1. An SS, Fabry B, Mellema M, Bursac P, Gerthoffer WT, Kayyali US, Gaestel M, Shore SA, Fredberg JJ. Role of heat shock protein 27 in cytoskeletal remodeling of the airway smooth muscle cell. J Appl Physiol 2004;96:1707–1713.
2. An SS, Laudadio RE, Lai J, Rogers RA, Fredberg JJ. Stiffness changes in cultured airway smooth muscle cells. Am J Physiol 2002;283:C792–C801.
3. An SS, Pennella CM, Gonnabathula A, Chen J, Wang N, Gaestel M, Hassoun PM, Fredberg JJ, Kayyali US. Hypoxia alters biophysical properties of endothelial cells via p38 MAPK- and Rho kinase-dependent pathways. Am J Physiol 2005;289:C521–C530.
4. Balaban NQ, Schwartz US, Riveline D, Goichberg P, Tzur G, Sabanay I, Mahalu D, Safran S, Bershadsky A, Addadi L, Geiger B. Force and focal adhesion assembly: a close relationship studied using elastic micropatterned substrates. Nature Cell Biol 2001;3:466–472. [PubMed: 11331874]
5. Besson A, Assoian RK, Roberts JM. Regulation of the cytoskeleton: an oncogenic function for CDK inhibitors. Nat Rev Cancer 2004;4:948–955. [PubMed: 15573116]
6. Bursac P, Lenormand G, Fabry B, Oliver M, Weitz DA, Viasnoff V, Butler JP, Fredberg JJ. Cytoskeletal remodeling and slow dynamics in the living cell. Nature Mat 2005;4:557–561.
7. Chicurel ME, Chen CS, Ingber DE. Cellular control lies in the balance of forces. Curr Opin Cell Biol 1998;10:232–239. [PubMed: 9561847]
8. Chou YH, Skalli O, Goldman RD. Intermediate filaments and cytoplasmic networking: new connections and more functions. Curr Opin Cell Biol 1997;9:49–53. [PubMed: 9013676]
9. Coughlin MF, Puig-de-Morales M, Bursac P, Mellema M, Millet E, Fredberg JJ. Filamin-A and rheological properties of cultured melanoma cells. Biophys J 2006;90:2199–2205. [PubMed: 16387775]
10. Crocker JC, Valentine MT, Weeks ER, Gisler T, Kaplan PD, Yodh AG, Weitz DA. Two-point microrheology of inhomogeneous soft materials. Phys Rev Lett 2000;85:888–891. [PubMed: 10991424]
11. Ellis RJ. Macromolecular crowding: an important but neglected aspect of the intracellular environment. Curr Opin Struct Biol 2001;11:114–119. [PubMed: 11179900]
12. Ellis RJ, Minton AP. Join the crowd. Nature 2003;425:27–28. [PubMed: 12955122]
13. Fabry B, Maksym GN, Butler JP, Glogauer M, Navajas D, Fredberg JJ. Scaling the microrheology of living cells. Phys Rev Lett 2001;87:148102. [PubMed: 11580676]
14. Felsenfeld DP, Choquet D, Sheetz MP. Ligand binding regulates the directed movement of beta 1 integrins on fibroblasts. Nature 1996;383:438–440. [PubMed: 8837776]
15. Forgacs G, Yook SH, Janmey PA, Jeong H, Burd CG. Role of the cytoskeleton in signaling networks. J Cell Sci 2004;117:2769–2775. [PubMed: 15150320]
16. Fuchs E, Cleveland DW. A structural scaffolding of intermediate filaments in health and disease. Science 1998;279:514–519. [PubMed: 9438837]
17. Gardel ML, Valentine MT, Crocker JC, Bausch AR, Weitz DA. Microrheology of entangled F-actin solution. Phys Rev Lett 2003;91:158302–1. [PubMed: 14611506]
18. Goodsell D. Biomolecules and nanotechnology. Am Scientist 2000;88:230–237.
19. Hu S, Chen J, Fabry B, Numaguchi Y, Gouldstone A, Ingber DE, Fredberg JJ, Butler JP, Wang N. Intracellular stress tomography reveals stress focusing and structural anisotropy in the cytoskeleton of living cells. Am J Physiol 2003;285:C1082–C1090.

20. Huang S, Ingber DE. The structural and mechanical complexity of cell-growth control. Nat Cell Biol 1999;1:E131–E138. [PubMed: 10559956]
21. Janmey PA. The cytoskeleton and cell signaling: component localization and mechanical coupling. Physiol Rev 1998;78:763–781. [PubMed: 9674694]
22. Klein U, Gimpl G, Fahrenholz F. Alteration of the myometrial plasma membrane cholesterol content with β-cyclodextrin modulates the binding affinity of the oxytocin receptor. Biochemistry 1995;34:13784–13793. [PubMed: 7577971]
23. Kubo R. Brownian motion and nonequilibrium statistical mechanics. Science 1986;233:330–334. [PubMed: 17737620]
24. Kuo KH, Wang L, Pare PD, Ford LE, Seow CY. Myosin thick filament lability induced by mechanical strain in airway smooth muscle. J Appl Physiol 2001;90:1811–1816. [PubMed: 11299271]
25. Lau AWC, Hoffman BD, Davies A, Crocker JC, Lubensky TC. Microrheology, stress fluctuations, and active behavior of living cells. Phys Rev Lett 2003;91:198101–1. [PubMed: 14611619]
26. Laudadio RE, Millet EJ, Fabry B, An SS, Butler JP, Fredberg JJ. Rat airway smooth muscle cell during actin modulation: rheology and glassy dynamics. Am J Physiol 2005;289:C1388–C1395.
27. Luna EJ, Hitt AL. Cytoskeleton-plasma membrane interactions. Science 1992;258:955–964. [PubMed: 1439807]
28. Mason TG, Gisler T, Kroy K, Frey E, Weitz DA. Rheology of F-actin solutions determined from thermally driven tracer motion. J Rheol 2000;44:917–928.
29. Maksym GN, Fabry B, Butler JP, Navajas D, Tschumperlin DJ, Laporte JD, Fredberg JJ. Mechanical properties of cultured human airway smooth muscle cells from 0.05 to 0.4 Hz. J Appl Physiol 2000;89:1619–1632. [PubMed: 11007604]
30. Matthews BD, Overby DR, Alenghat FJ, Karavitis J, Numaguchi Y, Allen PG, Ingber DE. Mechanical properties of individual focal adhesions probed with a magnetic microneedle. Biochem Biophys Res Commu 2004;313:758–764.
31. Mehta D, Gunst SJ. Actin polymerization stimulated by contractile activation regulates force development in canine tracheal smooth muscle. J Physiol 1999;519:829–840. [PubMed: 10457094]
32. Parker KK, Brock AL, Brangwynne C, Mannix RJ, Wang N, Ostuni E, Geisse NA, Adams JC, Whitesides GM, Ingber DE. Directional control of lamellipodia extension by constraining cell shape and orienting cell tractional forces. FASEB J 2002;16:1195–1204. [PubMed: 12153987]
33. Puig-de-Morales M, Millet E, Fabry B, Navajas D, Wang N, Butler JP, Fredberg JJ. Cytoskeletal mechanics in adherent human airway smooth muscle cells: probe specificity and scaling of protein-protein dynamics. Am J Physiol 2004;287:643–654.
34. Ramaekers FCS, Bosman FT. The cytoskeleton and disease. J Pathol 2004;204:351–354. [PubMed: 15495261]
35. Ritchie K, Shan XY, Kondo J, Iwasawa K, Fujiwara T, Kusumi A. Detection of non-Brownian diffusion in the cell membrane in single molecule tracking. Biophys J 2005;88:2266–2277. [PubMed: 15613635]
36. Riveline D, Zamir E, Balaban NQ, Schwarz US, Ishizaki T, Narumiya S, Kam Z, Geiger B, Bershadsky AD. Focal contacts as mechanosensors: externally applied local mechanical force induces growth of focal contacts by an mDial1-dependent and ROCK-independent mechanism. J Cell Biol 2001;153:1175–1185. [PubMed: 11402062]
37. Rolfe BE, Worth NF, World CJ, Campbell JH, Campbell GR. Rho and vascular disease. Atherosclerosis 2005;183:1–16. [PubMed: 15982657]
38. Schmidt CE, Horwitz AF, Lauffenburger DA, Sheetz MP. Integrin-cytoskeletal interactions in migrating fibroblasts are dynamic, asymmetric, and regulated. J Cell Biol 1993;123:977–991. [PubMed: 8227153]
39. Seow CY, Pratusevich VR, Ford LE. Series-to-parallel transition in the filament lattice of airway smooth muscle. J Appl Physiol 2000;89:869–876. [PubMed: 10956328]
40. Stamenovic D, Mijailovich SM, Tolic-Norrelykke IM, Chen J, Wang N. Cell prestress II. Contribution of microtubules. Am J Physiol 2002;282:C617–C624.
41. Suyama E, Wadhwa R, Kawasaki H, Yaguchi T, Kaul SC, Nakajima M, Taira K. LIM kinase-2 targeting as a possible anti-metastasis therapy. J Gene Med 2004;6:357–363. [PubMed: 15026997]

42. Tseng Y, Kole TP, Wirtz D. Micromechanical mapping of live cells by multiple-particle-tracking microrheology. Biophys J 2002;83:3162–3176. [PubMed: 12496086]

43. Wang N, Butler JP, Ingber DE. Mechanotransduction across the cell surface and through the cytoskeleton. Science 1993;260:1124–1127. [PubMed: 7684161]

44. Wang N, Tolic-Norrelykke IM, Chen J, Mijailovich SM, Butler JP, Fredberg JJ, Stamenovic D. Cell prestress I. Stiffness and prestress are closely associated in adherent contractile cells. Am J Physiol 2002;282:C606–C616.

45. Yamazaki D, Kurisu S, Takenawa T. Regulation of cancer cell motility through actin reorganization. Cancer Sci 2005;96:379–386. [PubMed: 16053508]

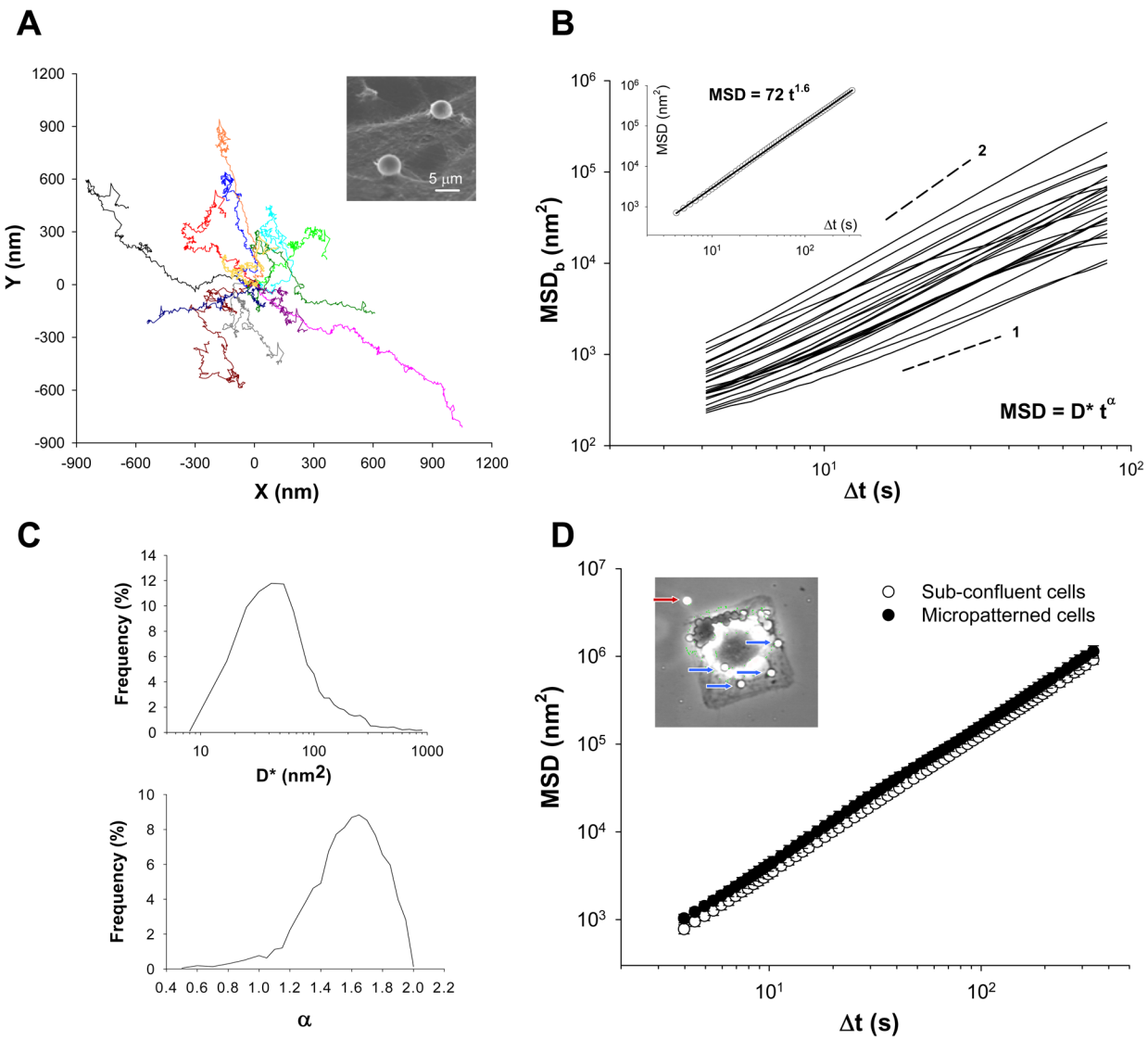

Figure 1. Characterization of spontaneous bead motions

A. Spontaneous motions of RGD-coated beads recorded over the course of 5 min. For clarity, only few representative tracings are depicted from the same point of origin (10 × objective, n = 14 beads). *Inset:* A scanning electron microphotograph of individual RGD-coated microbeads attached to the cell surface. **B.** Mean square displacement (MSD_b) calculated from Equation 1 are shown for representative beads. *Inset:* Ensemble average of all MSD_b (MSD) increased with time as ~ $t^{1.6}$. **C.** The histograms of diffusion coefficient D* and exponent α estimated from a least-square fits of a power-law (Equation 2) to the MSD_b data. **D.** MSD of beads on subconfluent cells (○) versus cells adhered to micropatterned substrates (●). *Inset:* RGD-coated microbeads (blue arrows) attached to a single micropatterned ASM cell (50 μm × 50 μm). Data are expressed as mean ± SE (n = 322 for beads on micropatterned and n = 1202 on sub-confluent cells).

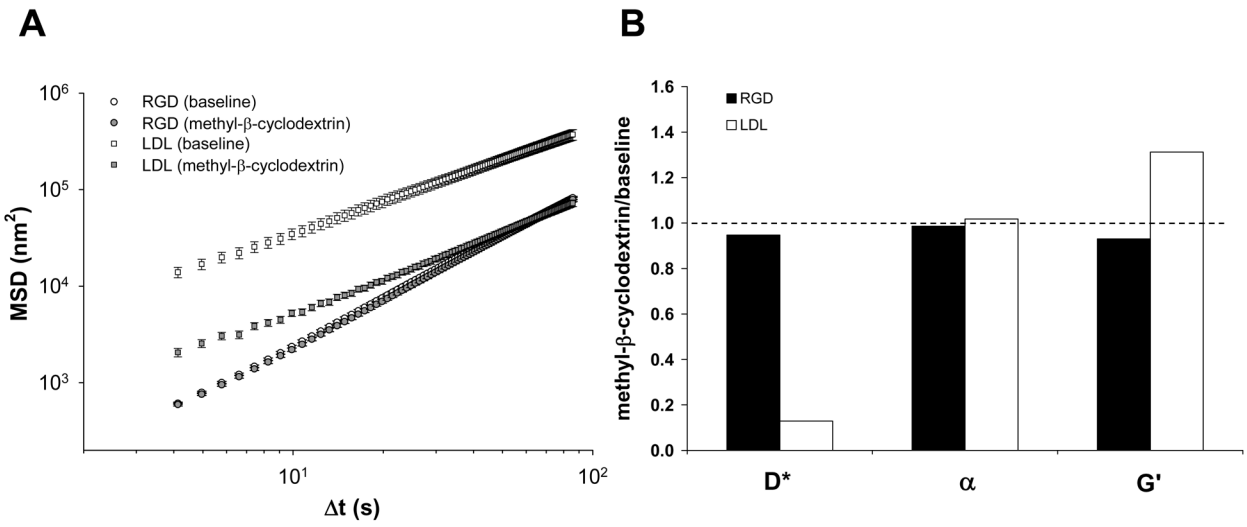

Figure 2. Role of lipid membrane dynamics

A. Addition of 10 mM methyl-β-cyclodextrin for 1 hr differentially affects MSD of beads coated with RGD [baseline (○) and treatment (Ï)] versus acLDL [beasline (□) and treatment (■)]. Data are mean ± SE (n = 2054 for RGD-coated and n = 887 for acLDL-coated beads). **B.** The effects of methyl-β-cyclodextrin on D*, α, and G′ are normalized to their respective baseline values.

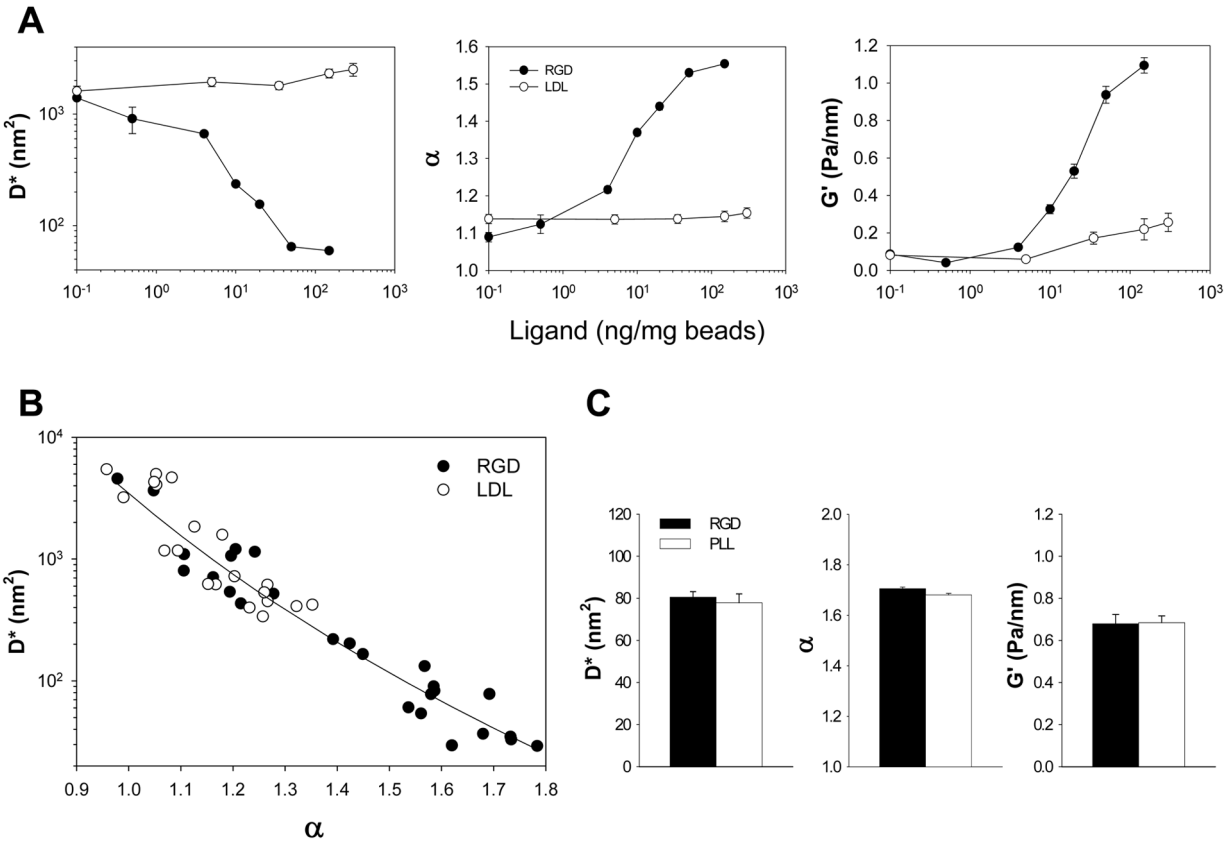

Figure 3. Ligand bead dynamics

A. Spontaneous (D* and α) and forced (G′) motions of individual microbeads (RGD versus acLDL) show distinct characteristics with respect to the ligand coating (0.1 to 300 ng/mg bead). Data are mean ± SE (n = 700 to 2500 beads). **B.** An inverse correlation between D* and α. Individual data points are ensemble averages of several hundred beads coated with different ligand concentrations and tested at different experimental days (data are taken from part A). **C.** D*, α, and G′ of individual microbeads (RGD versus PLL) attached to the cell surface. Data are mean ± SE (n = 1044 for RGD-coated and n = 1176 for PLL-coated beads).

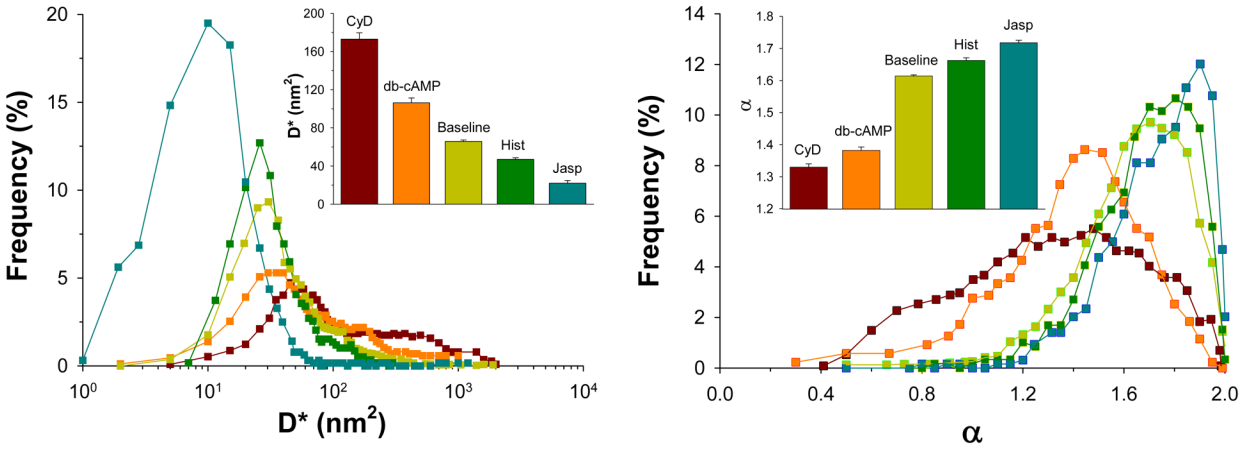

Figure 4. Anomalous bead motions correlate with changes in tension within the CSK

Histograms of D* and α were determined both before and after addition of jasplakinolide (Jasp, 1 μM; 10 min) and cytochalasin-D (CyD, 1 μM, 10 min) to modulate actin dynamics, and histamine (Hist, 100 μM; 5 min) and dibutryl-cAMP (db-cAMP, 1 mM; 15 min) to modulate myosin motors. Data are mean ± SE (n = 481 to 1174 beads).